2013 European Control Conference (ECC)
July 17-19, 2013, Zürich, Switzerland.

Predictive Control of Buildings for Demand Response with Dynamic Day-ahead and Real-time Prices

Evangelos Vrettos*, KuanLin Lai†, Frauke Oldewurtel* and Göran Andersson*

Abstract— **This paper proposes a Model Predictive Control (MPC) scheme to control residential buildings with space heating/cooling loads, an Electric Water Heater (EWH), photovoltaics (PV) and battery storage in a time-varying electricity price environment. The controller uses models for the system components as well as predictions for future disturbances such as weather conditions, occupancy and electricity prices to find the building operation that minimizes electricity costs over the prediction horizon while respecting user comfort constraints. The building operation is investigated under three different price scenarios: (1) a simple day-night tariff for end-customers, (2) a day-ahead dynamic tariff reflecting the wholesale market marginal costs and (3) a real-time dynamic tariff. Residential buildings response to such price signals is investigated in a case study and their potential for Demand Response (DR) programs is evaluated.**

I. INTRODUCTION

A. Background and Motivation

Power systems are facing new challenges due to increasing shares of Renewable Energy Sources (RES). RES are generally fluctuating in nature and introduce significant uncertainty in power system operation. Since storing electricity in bulk quantities is technically difficult and economically unattractive, the traditional paradigm of operation requires power production to follow the demand. However, the limited controllability of RES calls for additional flexibility in power systems, which can be provided by demand side resources.

Employing residential, commercial or industrial loads for power system control tasks is commonly referred to as Demand Response (DR). This paper is concerned with load shifting in residential buildings, which is a rather slow power system service with time constants in the order of a few hours. Load shifting can be implemented with price-based control, i.e., broadcasting of price signals as incentives for grid-friendly behavior. In [1] the potential and challenges of using loads for power system control actions are discussed and an overview of recent research in this field is presented. This paper defines a state-of-the-art benchmark of a residential building and investigates its potential for DR.

B. Related Work

The idea of using buildings for price-based DR applications is not new and a significant amount of related work can be found in literature. Some papers, such as [2]–[7], investigate how building aggregations can offer power system services including peak shaving, load shifting, power setpoint tracking and distribution network management. Other papers focus on optimal building control in a dynamic price environment. Since this paper falls in the second category in the following we summarize the important literature in this field.

In [8], a simple optimization model that allows a consumer to adapt its demand profile in response to electricity prices has been developed assuming all loads to be shiftable. A prototype that applies stochastic dynamic programming incorporating weather forecasts to minimize electricity costs by shifting heating/cooling loads and event-based loads (e.g., dishwashers) is presented in [9]. In [10], the authors develop a stochastic Model Predictive Control (MPC) strategy that uses a bilinear building model and takes into account weather predictions to increase energy efficiency. An MPC controller for building cooling systems equipped with thermal energy storage in water tanks has been proposed in [11], with the aim of achieving lower electricity costs. Reference [12] presents the practical implementation of an MPC controller for building thermal load management to stabilize fluctuations in the power grid due to high penetration of wind power. In [13] minimization of electricity costs for residential buildings with elastic demands, storage, local generation and real-time pricing is formulated as a stochastic optimization problem and approximately solved using the Lyapunov approach.

The aforementioned papers consider either time-varying prices that are known a priori, or real-time price signals as control inputs. However, the dependence of building flexibility for load shifting on the shape of price signals is not investigated. In addition, the effectiveness of employing real-time price control on top of day-ahead time-varying prices in a building with MPC controller is not examined. This paper explicitly addresses these two issues that are neglected in the literature.

C. Contribution

The contribution of this paper is threefold. First, it develops a state-of-the-art benchmark of a residential building with all installations for an efficient DR, namely Heat Pump (HP) for space heating, Slab Cooling (SC) for space cooling, Electric Water Heater (EWH), photovoltaics (PV) and battery storage. With this setup, the potential for electricity cost reduction in a dynamic end-customer electricity price environment using an MPC controller is investigated. Second, the paper provides a sensitivity analysis of the building response

*E. Vrettos, F. Oldewurtel and G. Andersson are with EEH-Power Systems Laboratory, Swiss Federal Institute of Technology (ETH) Zurich, 8092 Zurich, Switzerland (e-mail: {vrettos,oldewurtel,andersson}@eeh.ee.ethz.ch).

†K. Lai is a Master student at the Department of Electrical Engineering and Information Technology, Swiss Federal Institute of Technology (ETH) Zurich, 8092 Zurich, Switzerland (e-mail: klai@student.ethz.ch).

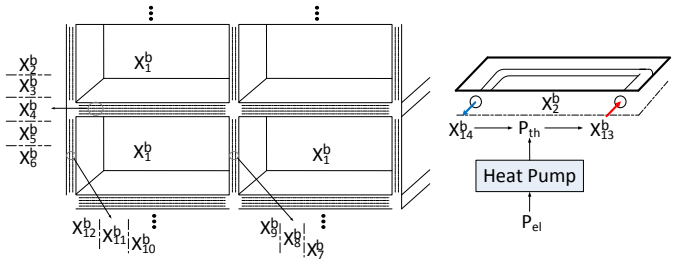

Fig. 1. Schematic representation of the building thermal model with the floor heating water system and the heat pump. States are the temperatures in the room, floor, walls, ceiling and water system.

with respect to day-ahead and real-time price signals. And third, it evaluates the potential of the residential building for DR schemes, in particular for the case where real-time price signals are superimposed on top of day-ahead price profiles.

The remainder of the paper is organized as follows. In Section II, the building dynamics are derived in state space form. In Section III, the MPC problem is formulated and in Section IV the considered building configurations and price signals for the case study are presented. Results are shown in Section V, while Section VI concludes the work.

II. COMPONENT MODELING

A. Building and Heat Pump Models

In this paper, a single room model based on developments within the OptiControl project [14], [15], is considered. The original model is based on a commonly used method that aggregates building zones in order to compute the building-wide energy use. The model has been validated by building experts and its dynamic response was found to match the relevant behavior of a building sufficiently [10].

The left hand side of Fig. 1 shows a schematic representation of the original building model that includes 14 states, representing the temperatures in the room and in different layers in floor, walls and ceiling. These layers are needed to model the heat transfer properties of different actuators, e.g., the fact that floor heating affects the room temperature with some delay. The basic model has been altered in two ways: first, it is augmented by introducing a HP that heats up water which is used for the TABS[2] system (see Fig. 1). The purpose of this augmentation is to better capture the dynamics between the HP and the TABS system. Second, the model has been simplified by neglecting lighting, blind positioning and ventilation.

The HP is modeled by the Coefficient of Performance (COP), i.e., the ratio of the output thermal power P_{th} to the input electric power P_{el}. In general, the COP is a function of the ambient temperature T_{amb} and the water supply temperature $T_{\text{w,s}}$. In this paper, a linear function is assumed as in [16] resulting in the following equations for COP and P_{th}:

[2]TABS = Thermally Activated Building System, i.e. the building is equipped with embedded tube-systems inside the floor, wall, or ceiling for heating and cooling.

$$COP = c_0 + c_1 T_{\text{amb}} + c_2 T_{\text{w,s}} \tag{1}$$

$$P_{\text{th}} = (c_0 + c_1 T_{\text{amb}} + c_2 T_{\text{w,s}}) \cdot P_{\text{el}} \quad , \tag{2}$$

where $c_0 = 5.593$, $c_1 = 0.0569\text{K}^{-1}$ and $c_2 = -0.0661\text{K}^{-1}$.

Since P_{el}, which is an input, depends on $T_{\text{w,s}}$, which is a state, HP dynamics are nonlinear. To keep the resulting MPC problem convex, HP dynamics are linearized by fixing $T_{\text{w,s}}$ in (1) to its steady state value assuming that all disturbances over the prediction horizon take their expected values and using a mixed cost function comprising a linear penalty for electricity cost and a quadratic penalty for P_{el}, as given in Section III-B. The resulting convex optimization problem was shown to be a good approximation of the original one in [16].

Building thermal dynamics can be seen as a circuit of first-order Ordinary Differential Equations (ODEs) representing heat transfer among the nodes in Fig. 1 and heating/cooling actuators. By aggregating ODEs for all nodes and discretizing we obtain the building dynamics in state space form:

$$x^{\text{b}}_{k+1} = A^{\text{b}} x^{\text{b}}_k + B^{\text{b}}_u u^{\text{b}}_k + B^{\text{b}}_v v^{\text{b}}_k \quad , \tag{3}$$

where $x^{\text{b}}_k \in \mathbb{R}^{14}$ is the building state vector, $u^{\text{b}}_k \in \mathbb{R}^2$ is the input vector comprising HP and SC electric power and $v^{\text{b}}_k \in \mathbb{R}^5$ is the disturbance vector comprising outside air temperature, wetbulb temperature, solar radiation, and internal gains from people and equipment. The reader is referred to [14], [15] for the detailed derivation of matrices A^{b}, B^{b}_u and B^{b}_v.

B. Electric Water Heater Model

An EWH is considered as additional thermal storage component for DR. EWH modeling is based on [17], where a thermally stratified linear EWH model with ten water layers is derived by applying a numerical solution scheme to the Partial Differential Equation (PDE) that governs diffusive and convective heat transfer in the water tank:

$$x^{\text{wh}}_{k+1} = A^{\text{wh}}_k x^{\text{wh}}_k + B^{\text{wh}}_k u^{\text{wh}}_k \quad . \tag{4}$$

In (4) $x^{\text{wh}}_k \in \mathbb{R}^{12}$ is the state vector containing the temperatures of the ten water layers, the incoming water temperature and ambient temperature, and $u^{\text{wh}}_k \in \mathbb{R}$ is the input vector, i.e., the heating power. Note that the disturbance term, i.e., water draw rate, is incorporated into the state and input matrices A^{wh}_k and B^{wh}_k, which are time-varying as indicated by the subscripts [17].

In [17] a nonlinear water layer mixing model has been introduced to account for natural convection due to buoyancy, which is not modeled in (4). In this paper, a simplified model, based on the assumption that the heating element power is distributed among the water layers with weights depending on their position, is used instead to keep the overall MPC problem linear. However, the original nonlinear mixing model has been used as plant model for EWH state update.

C. Lead-acid Battery Model

For stationary storage applications lead-acid batteries are currently an attractive solution due to their low capital cost [18]. A variant of the Kinetic Battery Model (KiBaM), which was originally proposed in [19], is used to simulate a lead-acid battery in the building. KiBaM considers the battery as a two-well system, where the first well represents directly available energy and the second one contains chemically bound energy, which may become available at a limited rate. Although KiBaM includes sub-models for the capacity, voltage, charge transfer, losses and degradation, in this model variant, which has been applied before in [20], only the capacity and charge transfer sub-models are kept after some modifications.

By rearranging the capacity equations provided in [20] we obtain the discrete time battery dynamics in state space form as in (5) (see top of next page). In (5) E_k^1 is the available energy, E_k^2 is the bound energy, b_1 is the capacity ratio parameter, b_2 is the battery rate constant, $b_3 = 1 - b_1$, $b_4 = e^{-b_2 \Delta t}$, Δt is the sampling time, n_d (n_c) is the discharging (charging) efficiency, and P_k^d (P_k^c) is the discharge (charge) power at time step k. The battery dynamics can then be written in the more compact form:

$$x_{k+1}^{\mathrm{bat}} = A^{\mathrm{bat}} x_k^{\mathrm{bat}} + B^{\mathrm{bat}} u_k^{\mathrm{bat}} \quad , \tag{6}$$

where $x_k^{\mathrm{bat}} = [E_k^1 \;\; E_k^2]^{\mathrm{T}}$, $u_k^{\mathrm{bat}} = [P_k^\mathrm{d} \;\; P_k^\mathrm{c}]^{\mathrm{T}}$ and the matrices $A^{\mathrm{bat}}, B^{\mathrm{bat}}$ are defined by (5). By considering distinct inputs for charge and discharge power different charging and discharging efficiencies can be modeled.

D. Photovoltaic Model

To investigate the impact of flexible demand and storage on exploitation of local generation, a rooftop PV is considered. A simple PV model for panels equipped with a Maximum Power Point Tracking (MPPT) controlled DC/DC converter has been adopted from [21]. According to this model, the PV power output depends linearly on cell temperature and nonlinearly on solar radiation. Note that there is no dynamic system related to PV, rather the model is used just to pre-compute the PV power output.

E. Uncontrollable Building Loads

The electricity consumption of uncontrollable loads (UC), e.g., lighting, televisions, ovens, etc., is taken into account by using the data from [22]. The data include power measurements of different loads with a time resolution of one second from a typical household for the week 21-28 April 2011, which is repetitively used throughout the whole year. While this assumption is reasonable for most uncontrollable loads, such as television and oven, this is generally not the case for lighting, which has a strong seasonal dependence. However, seasonality effects on uncontrollable loads are neglected in this work due to lack of appropriate data.

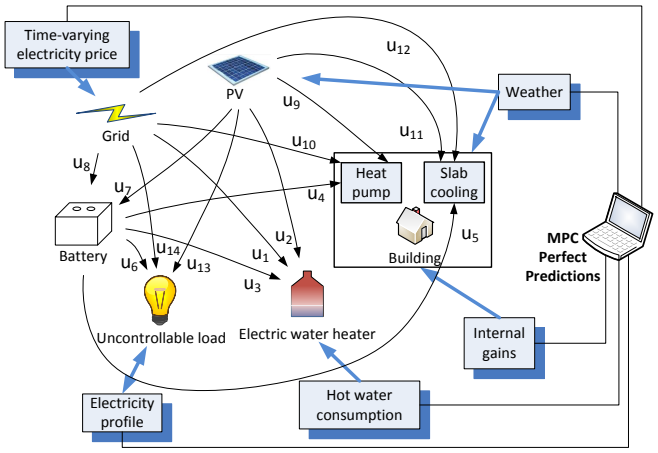

Fig. 2. Schematic representation of the system with all components and power flows among them.

F. External Inputs

External inputs to the building include weather data, internal heat gains due to people and equipment, and hot water consumption. The weather data comprise the outside air temperature, the wetbulb temperature and the incoming solar radiation and are taken from archived forecasts of the COSMO-7 numerical weather prediction model operated by MeteoSwiss. A residential building is considered in this work and it is assumed to be occupied from 6 pm each day till 7 am next day. Typical values for internal gains are taken from the Swiss standard SIA. A predefined probability profile of water draws from [17] is used to simulate daily hot water consumption, which is assumed equal to 280 liters.

G. Overall System Model

An overview of the whole system is given in Fig. 2. Note that for optimization purposes one has to distinguish the power sources, e.g., the power for the EWH can come either from the grid, from PV, or from the battery. The same holds for HP, SC, battery and uncontrollable loads. This is modeled by introducing separate control inputs (as can be seen in Fig. 2) and constraining the respective inputs to sum up to the total power input for the particular component. As Fig. 2 indicates, the PV power is consumed by the building loads rather than sold to the grid. The dynamics of the overall system containing all above components and separate control inputs are given by (7), where $x_k \in \mathbb{R}^{28}$, $u_k \in \mathbb{R}^{14}$ and $v_k \in \mathbb{R}^5$ are the overall system state, input and disturbance vectors, respectively:

$$x_{k+1} = A_k x_k + B_u u_k + B_v v_k \; . \tag{7}$$

III. CONTROLLER DESIGN

A. Rule-based Control

Rule-based Control (RBC) is the current practice in Building Automation Systems (BAS). As the name indicates, RBC determines actuators' control inputs based on a series of rules of the kind "if condition then action". In this paper, the conditions in RBC correspond to violation of state

$$\begin{pmatrix} E_{k+1}^1 \\ E_{k+1}^2 \end{pmatrix} = \begin{pmatrix} b_1+b_3b_4 & b_1(1-b_4) \\ b_3(1-b_4) & b_3+b_1b_4 \end{pmatrix} \cdot \begin{pmatrix} E_k^1 \\ E_k^2 \end{pmatrix} + \begin{pmatrix} \frac{b_3b_4+b_1(1-b_2\Delta t)-1}{b_2} \cdot \frac{1}{n_\mathrm{d}} & \frac{b_3b_4+b_1(1-b_2\Delta t)-1}{b_2} \cdot n_\mathrm{c} \\ \frac{-b_3(b_2\Delta t-1+b_4)}{b_2} \cdot \frac{1}{n_\mathrm{d}} & \frac{-b_3(b_2\Delta t-1+b_4)}{b_2} \cdot n_\mathrm{c} \end{pmatrix} \cdot \begin{pmatrix} P_k^\mathrm{d} \\ P_k^\mathrm{c} \end{pmatrix} \quad (5)$$

constraints, which are provided in Section III-B. RBC is used as a benchmark to assess the potential of electricity cost reduction by employing predictive control in BAS.

B. Model Predictive Control

The goal of MPC controller is to minimize electricity costs by using the developed building model and employing predictions for future disturbances, i.e., weather conditions, occupancy, hot water consumption and electricity prices, while respecting system constraints. In this work, perfect predictions of all disturbances are assumed. This simplifying assumption provides an upper bound for the expected improvement by predictive control.

The following state constraints on room temperature, average water tank temperature ($\bar{x}_k^{\mathrm{wh}}$) and battery State of Charge (SOC) are considered:

$$21 \leq x_{k,1}^{\mathrm{b}} \leq 23 \ [^\circ\mathrm{C}] \quad (8)$$

$$55 \leq \bar{x}_k^{\mathrm{wh}} \leq 70 \ [^\circ\mathrm{C}] \quad (9)$$

$$0.2 \cdot E_{\max} \leq E_k^1 + E_k^2 \leq E_{\max} = 5 \ [\mathrm{kWh}] \ . \quad (10)$$

Referring to the numbering adopted in Fig. 2, the input constraints can be written as follows:

$$0 \leq u_{k,i} \quad \forall\, i \in 1 \dots 14 \quad (11)$$

$$0 \leq u_{k,1} + u_{k,2} + u_{k,3} \leq P_{\mathrm{EWH}}^{\max} = 4.1 \quad (12)$$

$$0 \leq u_{k,3} + u_{k,4} + u_{k,5} + u_{k,6} \leq P_{\mathrm{Dmax},k}^{\mathrm{bat}} \quad (13)$$

$$0 \leq u_{k,7} + u_{k,8} \leq P_{\mathrm{Cmax},k}^{\mathrm{bat}} \quad (14)$$

$$0 \leq u_{k,4} + u_{k,9} + u_{k,10} \leq P_{\mathrm{HP}}^{\max} = 2 \quad (15)$$

$$0 \leq u_{k,5} + u_{k,11} + u_{k,12} \leq P_{\mathrm{SC}}^{\max} = 4 \quad (16)$$

$$0 \leq u_{k,2} + u_{k,7} + u_{k,9} + u_{k,11} + u_{k,13} \leq P_{\mathrm{PV},k} \quad (17)$$

$$P_{\mathrm{Dmax},k}^{\mathrm{bat}} = \xi_1^{\mathrm{T}} x_{k-1}^{\mathrm{bat}} \quad (18)$$

$$P_{\mathrm{Cmax},k}^{\mathrm{bat}} = \xi_2^{\mathrm{T}} x_{k-1}^{\mathrm{bat}} \quad (19)$$

$$P_{\mathrm{UC},k} = u_{k,6} + u_{k,13} + u_{k,14} \ , \quad (20)$$

where $P_{\mathrm{EWH}}^{\max}$ is the maximum EWH power, $P_{\mathrm{Dmax},k}^{\mathrm{bat}}$ and $P_{\mathrm{Cmax},k}^{\mathrm{bat}}$ are the maximum battery discharge and charge powers at time step k, respectively, $P_{\mathrm{HP}}^{\max}$ is the maximum HP power, $P_{\mathrm{SC}}^{\max}$ is the maximum SC power, $P_{\mathrm{PV},k}$ and $P_{\mathrm{UC},k}$ are the available PV power and the uncontrollable load, respectively, both at time step k. All inputs are given in kW. In (18) and (19) $\xi_1, \xi_2 \in \mathbb{R}^2$ are constant vectors that can be directly defined from the charge transfer model equations reported in [20].

Consider the prediction horizon N and define:

$$\mathbf{x} := [x_0^{\mathrm{T}}, \dots, x_N^{\mathrm{T}}]^{\mathrm{T}} \in \mathbb{R}^{28(N+1)} \quad (21)$$

$$\mathbf{u} := [u_0^{\mathrm{T}}, \dots, u_{N-1}^{\mathrm{T}}]^{\mathrm{T}} \in \mathbb{R}^{14N} \quad (22)$$

$$\mathbf{v} := [v_0^{\mathrm{T}}, \dots, v_{N-1}^{\mathrm{T}}]^{\mathrm{T}} \in \mathbb{R}^{5N} \ . \quad (23)$$

By adopting this notation the MPC problem can be formulated as follows:

$$\min_{\mathbf{u}} \quad w_0 \mathbf{c}^{\mathrm{T}}\mathbf{u} + w_1 \mathbf{u}^{\mathrm{T}}\mathbf{Q}\mathbf{u} + w_2(\mathbf{x} - \mathbf{T}_{\mathrm{ref}})^{\mathrm{T}}\mathbf{H}(\mathbf{x} - \mathbf{T}_{\mathrm{ref}}) \quad (24)$$

$$\text{s.t.} \quad \mathbf{S}\mathbf{u} \leq \mathbf{s} \quad (25)$$

$$\mathbf{G}\mathbf{x} \leq \mathbf{g} \quad (26)$$

$$\mathbf{F}\mathbf{x} = \mathbf{f} \quad (27)$$

$$\mathbf{x} = \mathbf{A}x_0 + \mathbf{B_u}\mathbf{u} + \mathbf{B_v}\mathbf{v} \ , \quad (28)$$

where $\mathbf{c} \in \mathbb{R}^{14N}$ denotes the electricity cost vector for the whole horizon, w_0, w_1, w_2 are weighting factors, and matrices $\mathbf{A}, \mathbf{B_u}, \mathbf{B_v}, \mathbf{S}, \mathbf{G}, \mathbf{F}$ and vectors $\mathbf{s}, \mathbf{g}, \mathbf{f}$ are of appropriate sizes.

The objective function in (24) consists of three terms: (a) a linear penalty representing the actual electricity cost, (b) a quadratic term penalizing the HP power and (c) a quadratic term penalizing room temperature deviations from a reference value. The entries of matrices $\mathbf{Q}$ and $\mathbf{H}$ take values in $\{0, 1\}$ such that the quadratic penalties are applied only to HP inputs, i.e., u_4, u_9 and u_{10} in Fig. 2, and room temperature deviations from the center of the comfort zone (22°C), respectively.

The three aforementioned terms are given different weights in (24). The quadratic penalty for HP power is required to linearize HP dynamics (see Section II-A). By incorporating the penalty for room temperature deviations an average annual temperature close to 22°C can be achieved, which is also the average annual temperature in case of RBC. This ensures that MPC energy and cost savings are due to prediction of disturbances and not due to compromise on user comfort, thus direct comparisons between MPC and RBC are possible. The weighting factors have been tuned to achieve a good tradeoff among cost minimization, smooth HP operation and reference temperature tracking. It was found out that the selection $w_0 = 1$, $w_1 = 0.2$ and $w_2 = 0.2$ results in reasonable operation. Assigning a significantly higher value to w_1 will penalize the HP power more and will eventually result in spreading its operation during the day, thus drastically reducing the potential for load shifting. Similarly, a much greater w_2 value will penalize aggressively even small temperature deviations from 22°C and will limit the potential for load shifting.

The optimization was performed with an hourly time step and a prediction horizon of 16 hours, which was found to be appropriate since longer horizons did not lead to significant cost reduction. Each optimization problem is solved in 3 seconds on average using CPLEX through a YALMIP interface [25] in a 4 core machine (2.83 GHz) with 8 GB RAM. Due

TABLE I

BUILDING CONFIGURATIONS

Component	Case I	Case II	Case III	Case IV
PV	-	-	✓	✓
Battery	-	✓	-	✓

TABLE II

PRICE SIGNALS

	Case A	Case B	Case C
Price signal	day-night	day-ahead dynamic	real-time

to the short computation time, also shorter time steps and hence larger optimization problems are tractable.

IV. INVESTIGATION SETUP

A. Building Configurations

A Swiss-average residential building with an area of 100 m^2, heavy construction, low window area fraction and south facade orientation is considered. The building is equipped with a HP with nominal power 2 kW, a SC installation with nominal power 4 kW and an EWH with nominal power 4.1 kW. Depending on the considered case (see Table I), the building may additionally include 12 PV panels with nominal power 160 W each and a battery with capacity 5 kWh.

B. Price Signals

The building is controlled using price signals for energy purchases from the grid, i.e., vector $\mathbf{c}$ in (24). In this paper, three different price signals are considered as summarized in Table II. First, a simple day-night tariff is considered, which is the common practice today in many countries. The tariff from *Elektrizitätswerk der Stadt Zürich* (EWZ) is used here. The day tariff from Monday to Saturday (6h-22h) is 0.185 CHF/kWh, whereas the night tariff from Monday to Saturday (22h-6h) is 0.095 CHF/kWh, which is also the tariff on Sundays and public holidays [23]. Second, a day-ahead time-varying tariff reflecting the wholesale market marginal costs is considered, which is taken from [23]. This tariff is based on the Swiss spot market prices of 2009 and can be used to shift load towards hours with high expected RES infeeds when the marginal costs are lower. And third, real-time pricing is considered, i.e., instantaneous price changes occurring at delivery time. Such price signals can be used to manipulate the consumption of a building or, better, an aggregation of buildings in order to track a power reference signal. A potential application is mitigation of RES infeed prediction errors.

V. RESULTS

In this section, the performance of the proposed MPC scheme as well as the building flexibility to day-ahead and real-time dynamic prices are assessed.

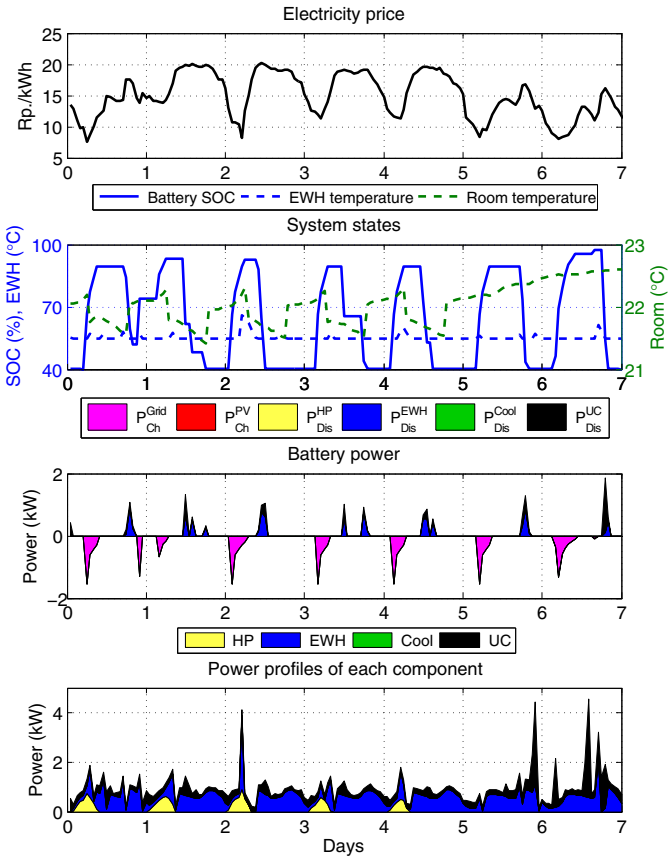

Fig. 3. Optimal building operation during a typical winter week [Case IV-B]. (a) Electricity price. (b) System states: room temperature, EWH average temperature and battery SOC. (c) Battery charge-discharge profile. (d) Power to controllable and uncontrollable loads.

A. System Operation with Day-ahead Dynamic Tariffs

Fig. 3 and Fig. 4 depict the optimal building operation for Case IV-B during a typical week in winter and summer, respectively. It can be seen that HP and SC operation are shifted towards low-price intervals, thus the controller clearly exploits building's thermal inertia. Similarly, the battery charges when the price is low and supplies the load when the price is high. Note that battery charge power decreases as SOC approaches 100% due to the charge transfer constraints as in (19). Most of the EWH energy is shifted to low price intervals using the battery and not the thermal inertia of the EWH. However, when the spread between low-price and high-price is large enough, e.g., during the third day of the winter week, the EWH shifts its consumption by storing energy in its thermal mass. During the summer week, the PV production is so high that covers the controllable and uncontrollable load and the excess energy is stored in the battery.

The EWH clearly dominates electricity consumption in both weeks, whereas the shares of HP and SC are significantly smaller. Even during the summer week there is little need for cooling since the average ambient temperature is around 20°C. Although the average ambient temperature during the winter week is approximately 5°C, the space

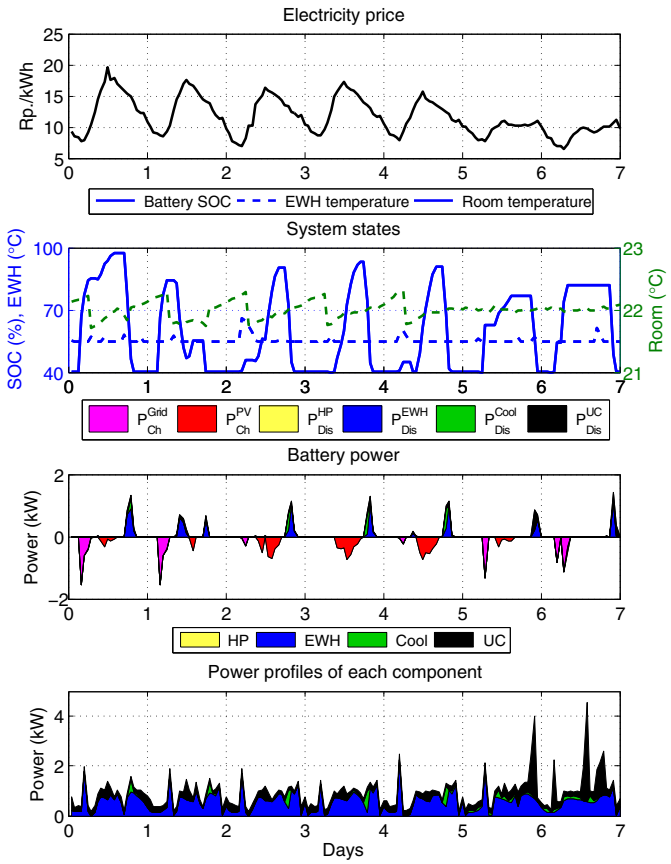

Fig. 4. Optimal building operation during a typical summer week [Case IV-B]. (a) Electricity price. (b) System states: room temperature, EWH average temperature and battery SOC. (c) Battery charge-discharge profile. (d) Power to controllable and uncontrollable loads.

heating needs are reduced due to the assumed high internal gains. The large impact of internal gains is evident during the weekend when there is no need for heating at all. In addition, the primary electricity consumption is further reduced due to the high COP of the HP, which is equal to 4.2 on average. On the other hand, the EWH consumes a lot of energy due to the high thermostat setpoints ($55-70°$C) and the assumed large hot water demand.

B. Potential for Electricity Cost Reduction

The potential of using MPC to minimize electricity costs in buildings was assessed considering all four building configurations and price cases A and B. Tables III and IV compare RBC and MPC in terms of annual electricity costs and energy consumption from the grid.

In cases I-A and I-B MPC reduces the cost by approximately 18% and the energy consumption by approximately 17% compared to RBC. The average room temperature for both control strategies is 22.07°C, whereas the average tank temperature is 55.52°C for MPC and 55.79°C for RBC. Therefore, the cost reduction indeed comes from exploiting predictions for disturbances and information about future prices but not from compromising on user comfort. By adding a battery to the system the additional savings in case of day-night tariff (case II.A) and day-ahead dynamic tariff

TABLE III

COMPARISON BETWEEN RBC AND MPC FOR CASE A.

Benchmark (RBC)				
	Electricity cost		Energy consumption	
	[CHF]	[%]	[kWh]	[%]
RBC: I-A, II-A	1426	-	9832	-
RBC: III-A, IV-A	1094	-	7882	-
Performance bound (MPC)				
	Electricity cost		Energy consumption	
	[CHF]	[%]	[kWh]	[%]
I-A	1170	-18.0	8123	-17.4
II-A	1129	-20.8	8413	-14.4
III-A	826	-24.5	6084	-22.8
IV-A	788	-28.0	6310	-19.9

TABLE IV

COMPARISON BETWEEN RBC AND MPC FOR CASE B.

Benchmark (RBC)				
	Electricity cost		Energy consumption	
	[CHF]	[%]	[kWh]	[%]
RBC: I-B, II-B	1448	-	9832	-
RBC: III-B, IV-B	1143	-	7882	-
Performance bound (MPC)				
	Electricity cost		Energy consumption	
	[CHF]	[%]	[kWh]	[%]
I-B	1181	-18.4	8170	-16.9
II-B	1133	-21.8	8427	-14.3
III-B	868	-24.1	6115	-22.4
IV-B	828	-27.6	6320	-19.8

(case II.B) are 2.8% and 3.4%, respectively. However, cost reduction comes with an increase in energy consumption of 3% in case II.A and 2.6% in case II.B, as compared to cases I.A and I.B, which is due to battery losses.

In a building with PV the benefits of using MPC are pronounced. In case III.A energy imports from the grid and costs decrease by 22.8% and 24.5%, respectively, whereas in case III.B the respective numbers are 22.4% and 24.1%. Therefore, the building thermal inertia can be efficiently used to increase local PV utilization in buildings. In this case the battery achieves additional savings of 3.5% in both price cases, which are slightly higher than before.

Based on these results a simple economic evaluation of battery installations in buildings for electricity cost reduction was carried out. By assuming a capital cost of 200 CHF/kWh for lead-acid batteries [18] and constant savings for every year equal to 49.2 CHF (which is the best case according to Table IV), the investment payback period is more than 20 years. Since typical battery lifetimes are 5-15 years [18], using batteries for this application is not economically viable with the current electricity price levels, battery efficiencies and capital costs.

C. Building Response to Day-ahead Price Signals

A sensitivity analysis has been carried out to investigate building response to day-ahead price signals during winter. The price for the next day is assumed to be a step of variable magnitude and duration starting at hour 10, as shown in Fig. 5. Hour 10 has been chosen as the starting time of the

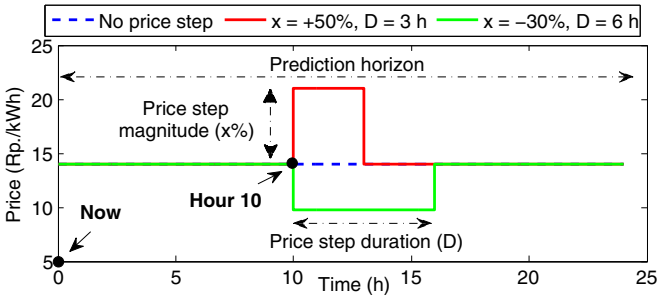

Fig. 5. Explanation of sensitivity analysis.

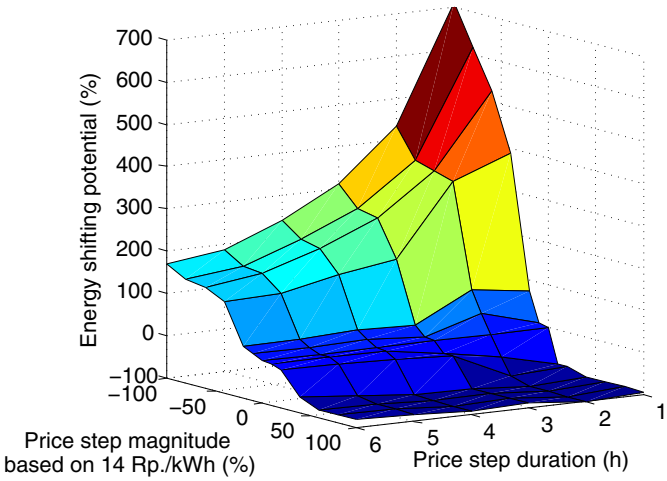

Fig. 6. Energy shifting potential as a function of magnitude and duration of day-ahead price steps (Case IV).

price step because then both the HP and the EWH would normally operate. The results of the sensitivity analysis for Case IV are shown in Fig. 6, where the energy shifting potential is defined as the consumption during the price step over the consumption without any price step.

A first observation is that percentage-wise the building is more responsive to negative than positive price steps, in particular if the duration of the negative price step is relatively short. Interestingly, most of the energy shifting potential can be achieved by a price step with duration of up to 2 hours. For a -100% price step and a duration of 1 hour the energy consumption increases by a factor of 7, whereas for a +100% price step and a duration of 1 hour the energy consumption decreases by approximately 93%. This means that the building is very sensitive to price signals that are known a priori, e.g., day-ahead. Another observation is that for price steps with a magnitude less than 30% the energy is shifted by using only the building and EWH thermal inertia. For larger price steps battery storage is also used since the battery roundtrip efficiency is around 74% including converter losses.

D. Building Response to Real-time Price Signals

Here, the term real-time price signal refers to a signal that is sent to the building only at the time when delivery of energy takes place, i.e., it is not known a priori like

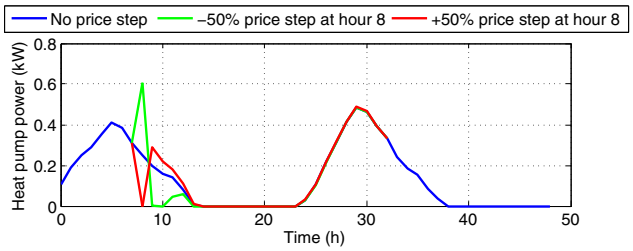

Fig. 7. HP Response to -50% and +50% real-time price signals.

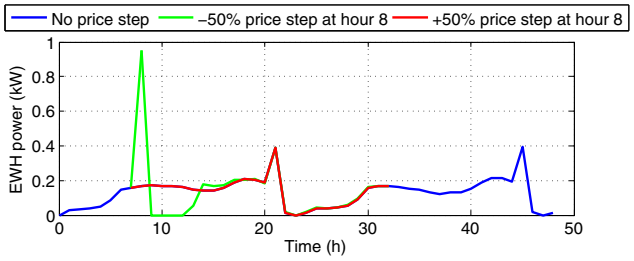

Fig. 8. EWH Response to -50% and +50% real-time price signals.

in Section V-C. In this paper, we assume that a particular building uses the developed MPC controller to optimize its operation based on price profiles that are communicated day-ahead. However, during physical delivery additional price signals may be superimposed on the day-ahead prices.

Fig. 7 and Fig. 8 depict the HP and EWH response, respectively, to a -50% and a +50% price signal occurring at hour 8. Both HP and EWH are able to respond to negative price signals by instantly increasing their consumption and shifting energy from subsequent hours. However, the behavior is different when it comes to positive price signals. The HP is able to switch off during hour 8 and compensate by increasing its consumption in the following 5 hours, whereas the EWH is not able to modify its consumption at all due to its faster dynamics and lower thermal inertia. Although these results are just for hour 8, a similar behavior was observed for any hour when both the HP and the EWH would normally operate. Of course, positive (negative) price signals occurring at times when the consumption is zero (maximum) will not affect the building behavior. The analysis indicates that both HP and EWH can contribute to real-time up regulation, however, only HP can effectively contribute to real-time down regulation. Note that the HP potential for down regulation depends heavily on the weighting factor w_2 in (24), that is the better the tracking of 22°C, i.e., staying in the middle of the comfort zone, the higher the potential.

By repeating the same analysis for several price steps in the range [-100%,100%] and aggregating the responses of all components, the building demand-price curves as in Fig. 9 can be derived. This figure shows how much the building consumption for the following hours will change if a real-time price signal is sent at hour 8. For the building under consideration, real-time price signals modify consumption up to 6 hours in the future. Again, it is obvious that the effect of negative price signals on consumption is much higher

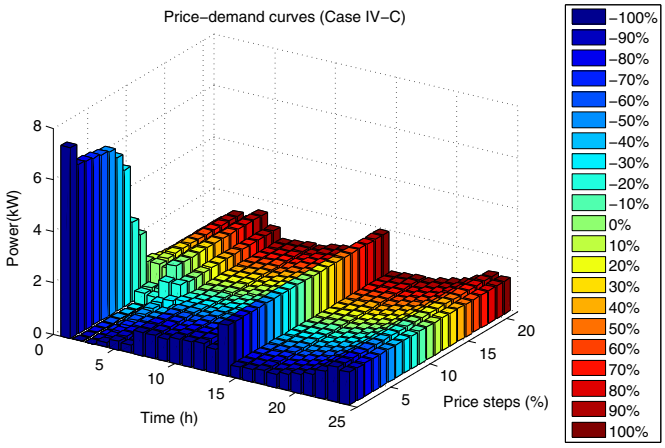

Fig. 9. Building demand-price curves for real-time price signals at hour 8 (Case IV-C). The curves show the sensitivity of demand on the magnitude of the price signal.

than that of positive price signals. Price-demand curves of different buildings can be used by load aggregators to incorporate the economic value of electricity for end-users in power markets, as in [24], or to minimize balancing energy costs due to RES infeed prediction errors.

VI. CONCLUSION

In this paper, a state-of-the-art benchmark of a residential building with a heat pump, slab cooling, an electric water heater, lead-acid battery storage, and photovoltaic panels for an efficient DR has been developed. An MPC controller that enables optimization of building operation in the presence of both day-ahead and real-time prices was proposed. A methodology for analyzing the building response to such price signals was introduced, which revealed a significant potential for DR. Apart from offering services to the power system, the proposed controller has the potential to achieve electricity cost savings for the building owner. Further studies have to investigate the potential in presence of more realistic (i.e. non-perfect) weather and occupancy predictions.

REFERENCES

[1] D.S. Callaway, and I.A. Hiskens, Achieving Controllability of Electric Loads, Proceedings of the IEEE, vol. 99, no. 1, pp. 184-199, Jan. 2011.

[2] D. L. Ha, F. Frizon de Lamotte, and Q. H. Huynh Real-time dynamic multilevel optimization for demand-side load management, presented at the IEEE International Conference on Industrial Enginnering and Engineering Management, Singapore, Dec. 2007, pp. 945-949.

[3] N. Li, L. Chen, S.H. Low, Optimal Demand Response Based on Utility Maximization in Power Networks, presented at IEEE PES General Meeting, Detroit, Michigan, USA, July 2011, pp. 1-8.

[4] T. Cui, H. Goudarzi, S. Hatami, S. Nazarian, and M. Pedram, Concurrent Optimization of Consumers Electrical Energy Bill and Producers Power Generation Cost under a Dynamic Pricing Model, presented at IEEE PES Conference on Innovative Smart Grid Technologies (ISGT), District of Columbia, USA, Jan. 2012, pp. 1-6.

[5] A. Molderink, V. Bakker, M. G. C. Bosman, J. L. Hurink, and G. J. M. Smit. Management and Control of Domestic Smart Grid Technology, IEEE Trans. on Smart Grid, vol. 1, no. 2, pp. 109-119, Sept. 2010.

[6] F. Oldewurtel, A. Ulbig, A. Parisio, G. Andersson, and M. Morari, Reducing Peak Electricity Demand in Building Climate Control using Real-Time Pricing and Model Predictive Control, presented at the 49th IEEE Conference on Decision and Control, Atlanta, Georgia, USA, Dec. 2010.

[7] F. Oldewurtel, A. Ulbig, M. Morari, and G. Andersson, Building Control and Storage Management with Dynamic Tariffs for Shaping Demand Response, presented at IEEE PES Conference on Innovative Smart Grid Technologies (ISGT) Europe, Manchester, UK, Dec. 2011.

[8] A. J. Conejo, J. M. Morales, and L. Baringo, Real-Time Demand Response Model, IEEE Trans. on Smart Grid, vol. 3, no. 3, pp. 236-242, December 2010.

[9] D. J. Livengood, The Energy Box: Comparing Locally Automated Control Strategies of Residential Electricity Consumption under Uncertainty, Ph.D. dissertation, Engineering Systems Division, Massachusetts Institute of Technology, Cambridge, MA, 2011.

[10] F. Oldewurtel et al, Energy Efficient Building Climate Control using Stochastic Model Predictive Control and Weather Predictions, presented at the American Control Conference, Baltimore, USA, June 2010.

[11] Y. Ma, F. Borrelli, B. Hencey, B. Coffey, S. Bengea, and P. Haves, Model Predictive Control for the Operation of Building Cooling Systems, IEEE Trans. on Control Systems Technology, vol. 20, no. 3, May 2012.

[12] Y. Zong, D. Kullmann, A. Thavlov, O. Gehrke, and H. W. Bindner, Application of Model Predictive Control for Active Load Management in a Distributed Power System With High Wind Penetration, IEEE Trans. on Smart Grid, vol. 3, no. 2, pp. 1055-1062, June 2012.

[13] Y. Guo, M. Pan, and Y. Fang, Optimal power management of residential customers in the smart grid, IEEE Trans. on Parallel and Distributed Systems, vol. 23, no. 9, pp. 1593-1606, Sept. 2012.

[14] D. Gyalistras et al., Use of weather and occupancy forecasts for optimal building climate control (OptiControl): Two years progress report, ETH Zurich and Siemens Building Technologies, 2009.

[15] F. Oldewurtel, Stochastic model predictive control for energy efficient building climate control, PhD Thesis, ETH Zrich, Switzerland, 2011.

[16] C. Verhelst, D. Axehill, C.N Jones, and L. Helsen, Impact of the cost function in the optimal control formulation for an air-to-water heat pump system, presented at 8th International Conference on System Simulation in Buildings (SSB), Liege, Belgium, Dec. 2010.

[17] E. Vrettos, S. Koch, and G. Andersson, Load Frequency Control by Aggregations of Thermally Stratified Electric Water Heaters, presented at the 3rd IEEE PES Innovative Smart Grid Technologies Europe (ISGT Europe), Berlin, Germany, Oct. 2012.

[18] H. Chen, T. N. Cong, W. Yang et al., Progress in Electrical Energy Storage System: A Critical Review, Progress in Natural Science, vol. 19, no. 3, pp. 291312, Mar. 2009.

[19] J.F. Manwell, and J.G. McGowan, Lead acid battery storage model for hybrid energy systems, Solar Energy, vol. 50, no. 5, pp. 399-405, May 1993.

[20] E. I. Vrettos, and S. A. Papathanassiou, Operating Policy and Optimal Sizing of a High Penetration RES-BESS System for Small Isolated Grids, IEEE Trans. on Energy Conversion, vol. 26, no. 3, pp. 744-756, Sept. 2011.

[21] H. Fakham, P. Degobert, and B. Francois, Control system and power management for a PV based generation unit including batteries, presented at Int. Aegean Conf. on Electrical Machines and Power Electronics (ACEMP 07), Bodrum, Turkey, Sept. 2007.

[22] J. Zico Kolter, and Matthew J. Johnson, REDD: A public data set for energy disaggregation research, prsented at the SustKDD workshop on Data Mining Applications in Sustainability, San Diego, USA, Aug. 2011.

[23] A. Ulbig, and G. Andersson, Towards variable end-consumer electricity tariffs reflecting marginal costs: A benchmark tariff, presented at the International Conference on the European Energy Market (EEM), Madrid, Spain, June 2010.

[24] Jhi-Young Joo, and M. Ilic, Adaptive load management (ALM) in electric power systems, presented at the International Conference on Networking, Sensing and Control (ICNSC), Chicago, USA, Apr. 2010.

[25] J. Löfberg, YALMIP: A toolbox for modeling and optimization in MATLAB, presented at the IEEE Conference on Computer-Aided Control Systems Design (CACSD), Taipei, Taiwan, Sept. 2004.